

ENERGY ACCEPTANCE AND ON MOMENTUM APERTURE OPTIMIZATION FOR THE SIRIUS PROJECT

P. S. Dester, F. H. de Sá, L. Liu*,
Brazilian Synchrotron Light Laboratory (LNLS), Campinas, Brazil

Abstract

A fast objective function to calculate Touschek lifetime and on momentum aperture is essential to explore the vast search space of strength of quadrupole and sextupole families in Sirius. Touschek lifetime is estimated by using the energy aperture (dynamic and physical), RF system parameters and driving terms. Non-linear induced betatron oscillations are considered to determine the energy aperture. On momentum aperture is estimated by using a chaos indicator and resonance crossing considerations. Touschek lifetime and on momentum aperture constitute the objective function, which was used in a multi-objective genetic algorithm to perform an optimization for Sirius.

INTRODUCTION

The adopted approach to optimize the non linear optics of Sirius storage ring is to use a Multi-Objective Genetic Algorithm, where the objective function is an estimator of on momentum aperture area and Touschek lifetime. Details about Sirius storage ring lattice can be found in [1] and [2]. On momentum aperture calculation is performed in key regions using chaos indicators, and energy acceptance calculation is performed using the concept of energy aperture (dynamic and physical). The Touschek lifetime is calculated through the energy acceptance. The idea is to have a fast algorithm to estimate the on momentum aperture area and Touschek lifetime, instead of performing a long and precise calculation, which in the case of the detailed lattice of Sirius takes around 7 hours. The goal is to take between 2 and 10 minutes per ring model. Therefore, we do not want to simulate lattice errors and correct them for each storage ring model tested, since it takes a considerable amount of time. Furthermore, for a lattice without errors, it is possible to take advantage of the five-fold symmetry in the Sirius optics, by simply using one superperiod for *tracking*. Regarding this strategy, care should be taken for 6D *tracking* to not change the synchrotron frequency nor the RF bucket. Our approach was to adjust the RF cavity frequency f_{RF} , so that $f_{RF} = k f_0$, where k is the harmonic number and f_0 is the revolution frequency in a superperiod.

To rigorously test a ring model, a set of twenty lattices with different configuration errors is generated. For each lattice, orbit, tune, coupling and symmetry are corrected. Then, on and off momentum apertures are carefully determined for each one of them. Throughout the paper, we always refer to this test when introducing lattice errors; the average of the results represents the estimation.

See Table 1 for definition of notations and symbols used in the paper. 4D map implies that cavity and radiation are not considered. When not explicitly stated, the derivative is implied to be with respect to the longitudinal position s . The majority of the calculations was performed with the MatLab Accelerator Toolbox.

Table 1: Notations and Symbols Used in the Paper

Symbol	Definitions/explanation
L	circumference (518.4 m)
s	$\in [0, L)$, longitudinal position
δ	energy deviation
τ	delay in respect to the synchrotron particle
β	energy dependant betatron function
ν	horizontal and vertical tunes
\mathbf{x}	$= (x, x', y, y', \delta, \tau)$, space coordinates
\mathbf{x}_{co}^{XD}	4D or 6D closed orbit coordinates
$\Phi_N^{XD}(\mathbf{x})$	N turns 4D or 6D map of a particle, \mathbf{x} represents the initial coordinates
$\ \cdot\ _2$	is the euclidean norm

ENERGY ACCEPTANCE CALCULATION

Let us define physical aperture A_{phys} as the smallest invariant betatron amplitude for which a particle with energy deviation δ collides with the vacuum chamber. Then,

$$A_{phys}(\delta) = \min_{s \in [0, L)} \left\{ \frac{(X_{VC}(s) - x_{co}^{4D}(s, \delta))^2}{\beta_x(s, \delta)} \right\}, \quad (1)$$

where X_{VC} is the vacuum chamber half-width.

Dynamic aperture represents the smallest invariant betatron amplitude for which the particle will eventually be lost. For the case of Sirius, where we do not have an x -plane symmetry, the calculation of dynamic aperture A_{dyn} is performed as follows

$$A_{dyn}(\delta) = \beta_x(s_0, \delta) \max_{x' \in \Omega(\delta)} \{(x' - x_{co}^{4D}(s_0, \delta))^2\}, \quad (2)$$

where $\Omega(\delta)$ is the greatest interval containing $x_{co}^{4D}(s_0, \delta)$ and satisfying

$$\Omega(\delta) \subset \{x' \in \mathbb{R} \mid \|\Phi_{\infty}^{6D}(x_{co}^{4D}, x', y_{co}^{4D}, y_{co}^{4D}, \delta, \tau_{co}^{6D})\|_2 < \infty\}$$

for a fixed longitudinal position s_0 , which in our case it was chosen in a straight section. All the above 4D closed orbit coordinates depend on s_0 and δ . $\|\Phi_{\infty}^{6D}(\mathbf{x})\|_2 < \infty$ means that the particle trajectory does not diverge. In practice, we used $N = 131$ turns for a rough estimation and $N = 900$

* E-mail: liu@lnls.br

for a more precise determination of A_{dyn} . The next step is to calculate the invariant betatron amplitude induced by Touschek scattering,

$$a_{\text{ind}}(s^*, \delta) = \frac{(\Delta x(s^*, \delta))^2}{\beta_x(s^*, \delta)} + \beta_x(s^*, \delta) \left(\Delta x'(s^*, \delta) - \frac{\beta'_x(s^*, \delta)}{2\beta_x(s^*, \delta)} \Delta x(s^*, \delta) \right)^2,$$

$\forall s^* \in [0, L]$, where $\Delta \mathbf{x}(s^*, \delta) = \mathbf{x}_{co}^{4D}(s^*, \delta) - \mathbf{x}_{co}^{6D}(s^*)$. A more detailed explanation of the equation used to calculate a_{ind} is discussed in [3]. For each s^* , we solve for δ ,

$$a_{\text{ind}}(s^*, \delta) = \min \left\{ A_{\text{dyn}}(\delta), \min_{\delta' \in [-\delta, \delta]} \{A_{\text{phys}}(\delta')\} \right\}. \quad (3)$$

Equation (3) has two solutions $\delta_i^+(s^*)$ and $\delta_i^-(s^*)$, which are the positive and negative local transverse acceptances, respectively. The overall energy acceptance is given by

$$\delta_{\text{acc}}^\pm(s) = \pm \min \{ \delta_{\text{RF}}, |\delta_w^\pm|, |\delta_i^\pm(s)| \}, \quad s \in [0, L], \quad (4)$$

where δ_{RF} is the acceptance of the RF system and δ_w^\pm is the energy deviation (positive and negative) for which the tune cross a resonance. An analogous approach to calculate energy acceptance is also used in [4]. Finally, Touschek lifetime is calculated by the method described in [5].

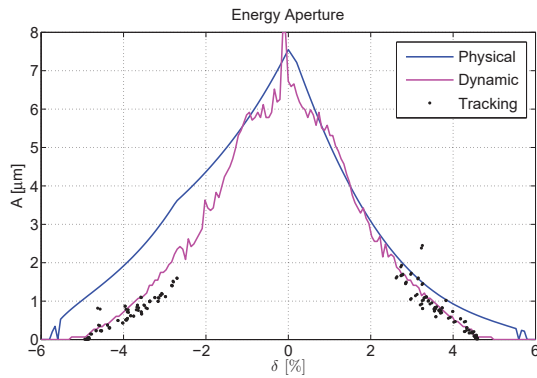


Figure 1: Dynamic and physical apertures for Sirius. The black dots correspond to the aperture calculated by tracking when lattice errors are introduced.

Figure 1 shows that the limiting aperture for Sirius is the dynamic aperture. Black dots represent the corresponding invariant betatron amplitude of a particle lost during *tracking* in the rigorous test with errors. In this case, the acceptance estimation is a good approximation of the Touschek acceptance. However, the method presented to calculate Touschek lifetime only guarantees an upper bound, which mostly is a satisfactory approximation.

ON MOMENTUM APERTURE CALCULATION

For Sirius project, the horizontal plane aperture at the negative side is important, since injection will occur at

ISBN 978-3-95450-182-3

$x \approx -8$ mm [6]. We use chaos indicators to estimate this aperture. When introducing errors in the lattice, particles in regions where there is a significant trace of chaos are usually lost. In this section, we compare the performance of two chaos indicators, the well known Diffusion and the proposed one ASDR (Average Square Distance Ratio).

Diffusion

Diffusion is calculated using NAFF (Numerical Analysis of Fundamental Frequencies) [7], a fast and precise algorithm to calculate fundamental frequencies of a motion. As it is explained in [8], let us denote NAFF by the operator $\mathcal{F}_N : \mathbf{x}_0 \mapsto \mathbf{v} - \lfloor \mathbf{v} \rfloor$. This operator calculates the fractional part of the horizontal and vertical tune, based on 4D *tracking* of N turns in the ring, starting from coordinate \mathbf{x}_0 . The diffusion vector is defined as

$$\mathbf{D} = \mathcal{F}_N(\mathbf{x}_0) - \mathcal{F}_N(\Phi_N^{4D}(\mathbf{x}_0)). \quad (5)$$

A chaos indicator is, then, given by $\|\mathbf{D}\|_2$. We observed that $\|\mathbf{D}\|_2 > 10^{-4}$ represents a significant probability of losing the particle, when lattice errors are introduced.

ASDR

Let $\{\mathbf{x}_{i,0}\}_{1 \leq i \leq M}$ be a set of initial conditions and $\mathbf{x}_{i,n} = \Phi_n^{4D}(\mathbf{x}_{i,0})$. Then, we define

$$\langle \Delta \zeta_{i,n}^2 \rangle_{0 \leq n \leq N} = \frac{1}{N+1} \sum_{n=0}^N (\zeta_{i+1,n} - \zeta_{i,n})^2,$$

for $1 \leq i < M$, where ζ represents any space coordinate in $\mathcal{R} = \{x, x', y, y'\}$. For example, $\zeta = x$, gives $x_{i,n}$, which is the horizontal position coordinate of the vector $\mathbf{x}_{i,n}$. Finally, the ASDR indicator is given by

$$\text{ASDR}_i^2 = \frac{1}{4 \#(\mathcal{R})} \sum_{\zeta \in \mathcal{R}} \frac{\langle \Delta \zeta_{i,n}^2 \rangle_{0 \leq n \leq 2N}}{\langle \Delta \zeta_{i,n}^2 \rangle_{0 \leq n \leq N}}, \quad (6)$$

where $\#(\mathcal{R}) = 4$ is the cardinality of \mathcal{R} . To simplify the analysis, let us consider only the horizontal dynamic, i. e., $\mathcal{R} = \{x, x'\}$. If (x, x') is of the form $(A_i \cos(\omega_i n + \phi_i), -A'_i \sin(\omega_i n + \phi_i))$, then one can show that

$$\text{ASDR}_i^2 = 1 - \frac{1}{4N} + o\left(N^2 \Delta \omega_i^2, \frac{1}{N}, \frac{\Delta A_i}{A_i}, \frac{\Delta A'_i}{A'_i}, \Delta \phi_i\right),$$

where $\Delta A_i = A_{i+1} - A_i$, $\Delta A'_i = A'_{i+1} - A'_i$, $\Delta \omega_i = \omega_{i+1} - \omega_i$ and $\Delta \phi_i = \phi_{i+1} - \phi_i$. Notice that we must have the successive initial conditions close to each other, in particular $\Delta \omega_i \ll 1/N \ll 1$; and β'_x must be small, in order to obtain a $\pi/2$ phase shift between x and x' , which allow us to cancel oscillating terms. Furthermore, $\omega_i/(2\pi)$ must be far from any integer, in order to the oscillating terms remain small. It is important to note that, if we are in a region where the frequency shift $\Delta \omega_i \ll (\Delta A_i/A_i)/N$, then $\text{ASDR}_i^2 \approx 1/4$.

Analogous reasoning can be done when added the vertical dynamics. For a well-behaved motion, it is expected that

05 Beam Dynamics and Electromagnetic Fields

$1/4 < \text{ASDR}_i^2 < 1$. Therefore, for sufficiently close initial conditions, $\text{ASDR}_i^2 > 1$ indicates a motion different from the one proposed, which suggests a chaotic behavior.

Comparison

We have compared the performance of chaos indicators over 62 ring models, on which we had already performed the rigorous test including errors. Figure 2 shows the Relative Mean Square Error (RMSE) of the indicator as a function of the chosen *threshold*. As expected, if the chaos indicator *threshold* is too small or too large, then the prediction fail.

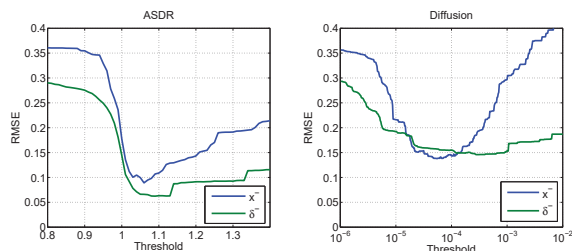


Figure 2: Blue and green curves correspond to RMSE of horizontal and energy negative apertures, respectively.

For both indicators the number of turns per initial condition was $N = 130$ and the step between initial conditions for x^- was $20 \mu\text{m}$ and for δ^- was $8.5 \cdot 10^{-5}$.

For this comparison, indicator ASDR with a relative error of approximately 10% at *threshold* around 1.05 performs better than Diffusion with a relative error of approximately 15% at *threshold* around 10^{-4} . In fact, we observed that for these *thresholds*, ASDR generally predicts a smaller aperture, which is more precise than Diffusion.

OPTIMIZATION RESULTS

The described methods to calculate energy acceptance and on momentum aperture are sufficient to form an objective function, which calculates Touschek lifetime τ_{TC} and on momentum aperture area $A_{x \times y}$, as a function of the ring model. This function takes between 2 to 10 minutes per model, while the standard technique takes around 7 hours. Let us represent the objective function as

$$f : \mathbb{R}^{N_S+2} \longrightarrow \mathbb{R}^2 \\ (\mathbf{S}, \nu) \longmapsto (\tau_{\text{TC}}, A_{x \times y}),$$

where \mathbf{S} is the vector of strength of sextupole families, $N_S = \dim(\mathbf{S})$ (In case of Sirius, $N_S = 21$) and the quadrupole strengths are calculated in order to reach the specified tunes ν with minimal modification. Singular Value Decomposition (SVD) was used to perform this task. This objective function is used in a Multi-Objective Genetic Algorithm (MOGA), which in our case was NSGA-II. A detailed explanation of this algorithm is given in [9].

To enhance search time, some restrictions are imposed, which are much faster to calculate than the objective-function. The feasible region was restricted to model rings with small positive chromaticity and a minimum upper

bound for Touschek lifetime, which is calculated using only the physical aperture, see Eq. (3). The gain is to provide a fast way to avoid rings which does not have the minimum lifetime required.

At certain point in the optimization of Sirius, NSGA-II was exploring solutions for which some *driving terms* (see [10]) were being increased to enhance on momentum aperture (h_{21000}, h_{30000}) or energy acceptance (h_{10110}), however when lattice errors were added, the particles did not survive. Therefore, these *driving terms* were added as constraints to remain smaller than a certain quantity. Thus, avoiding this kind of problems. Another strategic constraint we have added was a specific tune resonance of fourth order for the x -plane, which aided to predict the on momentum aperture, along with the chaos indicators.

The best results of the optimization, which were submitted to the rigorous test with errors are listed in Table 2, where we used a multi-bunch uniform filling operation mode, with 1% coupling and total current of 100 mA. Despite model R11G70M024 having a gain of 2.3 hours in Touschek lifetime, the loss in on momentum aperture may be risky for injection. The most safe result is model R11G16M019, where we have a significant gain in every aspect and a small standard deviation.

Table 2: Performance of Models

Model	$A_{x \times y}$ [mm ²]	x_{\min} [mm]	τ_{TC} [h]
original	40.0 ± 2.6	-10.0 ± 0.4	12.2 ± 0.4
R11G16M019	43.6 ± 1.6	-10.2 ± 0.4	13.4 ± 0.4
R11G23M017	42.0 ± 2.2	-10.4 ± 0.3	13.3 ± 0.4
R11G70M024	37.3 ± 2.3	-9.5 ± 0.8	14.5 ± 0.6
R13G38M018	38.9 ± 2.0	-11.0 ± 0.7	11.5 ± 0.7

CONCLUSION

Using the energy acceptance and on momentum aperture methods, we only had an upper bound estimation of the parameters. However, adding constraints related to *driving terms* and resonances, enhanced the methods to be reasonable approximations.

The best ranked machines from the optimization were selected to perform a rigorous test with lattice errors. Then, we could detect the best configuration models among them. These results are shown in Table 2.

The optimization method still needs improvement. The next step is to study the possibility of using another optimization algorithm with faster convergence than NSGA-II, for example the algorithm presented in [11].

ACKNOWLEDGMENTS

We thank Ximenes R. Resende for the suggestions and fruitful discussions; the reviewers for improving the readability of the paper; and the members of the LNLS Mechanical Design Group for conceding the spare time of their computers to our calculations.

REFERENCES

- [1] L. Liu, F. de Sá, and X. Resende, “A new optics for Sirius,” in *7th International Particle Accelerator Conference (IPAC'16)*, Busan, Korea, May 2016, pp. 3413–3416.
- [2] F. de Sá, L. Liu, and X. Resende, “Optimization of nonlinear dynamics for Sirius,” in *7th International Particle Accelerator Conference (IPAC'16)*, Busan, Korea, May 2016, pp. 3409–3412.
- [3] A. Nadji *et al.*, “Energy acceptance and touschek lifetime calculations for the SOLEIL project,” in *Particle Accelerator Conference*, vol. 2. IEEE, 1997, pp. 1517–1519.
- [4] H. Tsai *et al.*, “Energy acceptance and touschek lifetime calculations for the TPS storage ring,” in *IPAC'10*, 2011, pp. 2621–2623.
- [5] A. Piwinski, “The touschek effect in strong focusing storage rings,” *arXiv preprint physics/9903034*, 1999.
- [6] L. Liu, X. Resende, A. Rodrigues, and F. de Sá, “Injection dynamics for Sirius using a nonlinear kicker,” in *7th International Particle Accelerator Conference (IPAC'16)*, Busan, Korea, May 2016, pp. 3406–3408.
- [7] J. Laskar, “Introduction to frequency map analysis,” in *Hamiltonian systems with three or more degrees of freedom*. Springer, 1999, pp. 134–150.
- [8] Y. Papaphilippou, “Detecting chaos in particle accelerators through the frequency map analysis method,” *Chaos: An Interdisciplinary Journal of Nonlinear Science*, vol. 24, no. 2, p. 024412, 2014.
- [9] K. Deb, A. Pratap, S. Agarwal, and T. Meyarivan, “A fast and elitist multiobjective genetic algorithm: NSGA-II,” *IEEE transactions on evolutionary computation*, vol. 6, no. 2, pp. 182–197, 2002.
- [10] A. J. Dragt, *Lie methods for nonlinear dynamics with applications to accelerator physics*. University of Maryland, Center for Theoretical Physics, Department of Physics, 1997.
- [11] X. Huang and J. Safranek, “Online optimization of storage ring nonlinear beam dynamics,” *Physical Review Special Topics-Accelerators and Beams*, vol. 18, no. 8, p. 084001, 2015.